Solar Energy Materials & Solar Cells 215 (2020) 110592

Contents lists available at ScienceDirect

Solar Energy Materials and Solar Cells

journal homepage: http://www.elsevier.com/locate/solmat

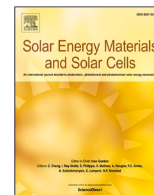

On the hydrogenation of Poly-Si passivating contacts by Al_2O_3 and SiN_x thin films

Bas W.H. van de Loo [a,1], Bart Macco [a,*,1], Manuel Schnabel [b], Maciej K. Stodolny [c], Agnes A. Mewe [c], David L. Young [b], William Nemeth [b], Paul Stradins [b], Wilhelmus M.M. Kessels [a]

[a] *Department of Applied Physics, Eindhoven University of Technology, P.O. Box 513, 5600, MB, Eindhoven, the Netherlands*
[b] *National Renewable Energy Laboratory, Golden, CO, 80401, USA*
[c] *ECN.TNO, P.O. Box 1, NL-1755, ZG, Petten, the Netherlands*

ARTICLE INFO

Keywords:
Hydrogen
Passivating contacts
Solar cells
Surface passivation
Polysilicon

ABSTRACT

Doped polycrystalline silicon (poly-Si), when coupled with a thin SiO_2 interlayer, is of large interest for crystalline silicon (*c*-Si) solar cells due to its outstanding passivating contact properties. To reach high levels of surface passivation, it is pivotal to hydrogenate the poly-Si and the underlying *c*-Si/SiO_2 interface. This can be done by capping the poly-Si with a hydrogen-containing dielectric layer such as Al_2O_3 or SiN_x, followed by a thermal anneal. On the basis of recent research, this work addresses several aspects of such hydrogenation by dielectric materials, including the effect of the annealing ambient, the thermal stability and reversibility of hydrogenation, the poly-Si doping level and *c*-Si surface texture. Additionally, the implementation of hydrogenation of poly-Si by dielectric materials in solar cells is discussed.

1. Introduction

Currently, there is tremendous interest within the crystalline silicon (*c*-Si) solar cell community in passivating contacts that are based on stacks of ultrathin SiO_2 and doped polycrystalline silicon (poly-Si). These poly-Si passivating contacts, that are also known by the abbreviations TOPCon [1] and POLO [2], have thus far led to *c*-Si solar cells with efficiencies as high as 25.7% and 26.1% on laboratory scale for both-side contacted and interdigitated back-contact (IBC) solar cells, respectively [1,2]. Moreover, poly-Si passivating contacts are currently being introduced in large-scale mass production [3].

The success of poly-Si passivating contacts can be understood from the extremely low contact resistivity ρ_c and recombination current density J_0 values that can be achieved, which together are the two main figures of merit for passivating contacts [4,5]. Reported values of J_0 and ρ_c are well below 10 fA/cm^2 and 1 mΩcm^2, respectively [1,6].

A cross-sectional transmission electron microscopy image of a typical poly-Si passivating contact structure is shown in Fig. 1. Manufacturing of such passivating contact is in fact very versatile as the various components can be effectively prepared in many different ways. Firstly, the ultra-thin SiO_2 oxide can be formed by e.g., thermal-, UV-ozone-, or wet-chemical oxidation of the c-Si surface [7,8]. Next, the poly-Si is typically prepared using low-pressure chemical vapor deposition (LP-CVD) or by plasma-enhanced CVD (PE-CVD) of hydrogenated amorphous silicon (*a*-Si:H) followed by solid-phase crystallization (SPC) [1,2,9,10]. The *n*- or *p*-type doping of poly-Si, required to achieve selective extraction of respectively electrons or holes from the c-Si bulk, can be realized *in-situ*, by admixing dopant gases during deposition, or *ex-situ*, through diffusion or by ion-implantation of dopants [11–14]. For ion-implantation or in-situ-doped poly-Si, a subsequent high-temperature anneal (typically above 850 °C) is required to activate the dopants [14].

Finally, to further improve the levels of surface passivation provided by the poly-Si, it is crucial to passivate electronically active Si dangling bonds at the *c*-Si/SiO_2 interface by *hydrogenation* [15]. Since the poly-Si is devoid of hydrogen after preparation, typically an external source of hydrogen is needed. This hydrogenation step can be realized in several different ways as well. Feldmann *et al.*, have achieved hydrogenation of poly-Si contacts by exposing them to a remote hydrogen plasma [16,17]. Furthermore, hydrogenation of poly-Si can also be achieved by having a hydrogen-containing capping layer on top of the poly-Si, such as Al_2O_3, SiN_x, or a transparent conductive oxide (TCO), typically prepared by atomic layer deposition (ALD), PE-CVD or sputtering, followed by a

* Corresponding author.
E-mail address: b.macco@tue.nl (B. Macco).
[1] B.W.H. van de Loo and B. Macco contributed equally to this work.

https://doi.org/10.1016/j.solmat.2020.110592
Received 18 September 2019; Received in revised form 24 April 2020; Accepted 4 May 2020
Available online 19 May 2020
0927-0248/© 2020 The Authors. Published by Elsevier B.V. This is an open access article under the CC BY license (http://creativecommons.org/licenses/by/4.0/).

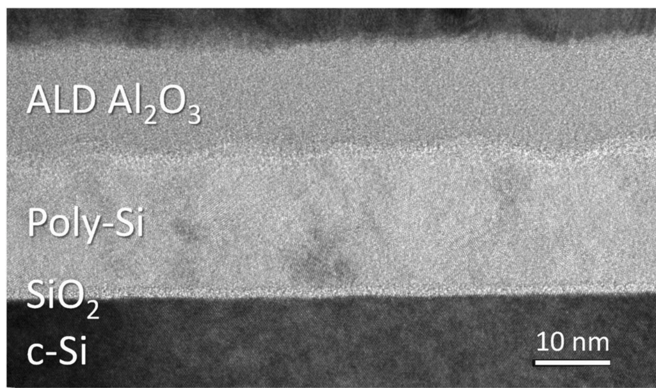

Fig. 1. High-resolution cross-sectional transmission electron microscopy image of a typical c-Si/SiO_2/poly-Si/Al_2O_3 passivating contact structure on top of *c*-Si. The SiO_2 was prepared by thermal oxidation, whereas the p^+ poly-Si was prepared by in-situ doped PE-CVD. The 30-nm thick Al_2O_3 capping layer, prepared by atomic layer deposition, provides hydrogen to the *c*-Si/SiO_2 interface during the anneal.

thermal annealing step [9,18,19]. Such hydrogenation step is reminiscent of e.g., the hydrogenation of the *c*-Si/SiO_2 interface by Al_2O_3 and a subsequent anneal [20]. There, the Al_2O_3 serves two purposes: *i)* it is a source of hydrogen for the hydrogenation, and *ii)* it retains the hydrogen in the underlying film. Notably, the importance of hydrogenation of poly-Si passivating contacts has also been observed by other research groups in the last few years [21–28].

In this work, we provide an overview of recent insights regarding the hydrogenation of poly-Si passivating contacts through dielectric materials. To this end, experimental results that have been obtained on a variety of different types of poly-Si passivating contacts, e.g., *p*- and *n*-type poly-Si prepared by LP- and PE-CVD are used. The overview draws from insights that have been published elsewhere as well as from our own recent work.

Specifically, first the mechanism behind hydrogenation and the accompanied improvement in *chemical* passivation is discussed. Subsequently, it is shown how Al_2O_3 and SiN_x dielectric layers can strongly improve the thermal stability of the contacts and that these layers can be removed after hydrogenation without impairing the improved lifetime. Also, the process of hydrogenation is shown to be completely reversible. Next, the role of the poly-Si doping level is discussed. Finally, we will discuss the implementation of hydrogenation of poly-Si by a dielectric material in solar cells.

2. Experimental details

The samples studied in this work consist of symmetrically-passivated lifetime samples. *n*-type CZ-grown wafers were used as substrates. Thermal oxidation was carried out to form a tunnel oxide. PE-CVD *a*-Si:H layers were *in-situ* B-doped and post-deposition crystallized by annealing in N_2 at 850 °C for 30 min. LP-CVD was used to grow intrinsic poly-Si, which were subsequently *ex-situ* doped by $POCl_3$-or BBr_3-diffusion. LP-CVD and doping were both performed in a Tempress System tube furnace. ALD Al_2O_3 layers were grown at 200 °C using trimethylaluminum (TMA) and H_2O as precursors. ALD layers were either grown by temporal ALD in an Oxford Instruments OpAL reactor or by spatial ALD using a Levitrack system of Levitech. Silicon nitride depositions were performed by PE-CVD in a MAiA tool of Meyer Burger. Selected samples received a few second firing treatment on a firing belt at various firing temperatures.

The level of surface passivation was evaluated by quasi-steady-state photoconductance decay (QSSPC) measurements using a Sinton lifetime tester. The implied open-circuit voltage (iV_{oc}) was evaluated at one sun illumination, whereas the J_0 values were extracted using the method of Kane and Swanson [29]. The doping level of the poly-Si was determined by electrochemical capacitance-voltage (ECV) profiling (WEP wafer profiler, CVP21). SIMS profiling was performed using a Cameca IMS 7f instrument. The resulting profiles were quantified using implanted Si standards. It should therefore be noted that the reported hydrogen concentration is calibrated in the poly-Si and the *c*-Si wafer but not per se in the Al_2O_3 layer.

3. Principles of the hydrogenation of poly-Si by dielectrics

The importance of hydrogenation in attaining a high level of surface passivation is demonstrated in Fig. 2, which shows the iV_{oc} of an *n*-type c-Si wafer passivated on both sides by p^+ poly-Si contact. As can be seen, the passivation level of as-deposited poly-Si can be enhanced by thermal annealing. Although the passivation is enhanced slightly by annealing in N_2, it can be further enhanced by annealing in forming gas (FGA). The higher passivation level that is achieved when annealing in forming gas indicates that hydrogen plays a role in the surface passivation. Interestingly, much higher surface passivation levels can be achieved when 30-nm of Al_2O_3 is deposited on top of the poly-Si, followed by a thermal anneal. In this case, the final passivation level is much less dependent on the annealing ambient as similar levels of passivation are achieved when annealing in an N_2 or forming gas ambient.

The mechanism behind the effective hydrogenation from ALD Al_2O_3 can be visualized from secondary ion-mass spectrometry (SIMS) measurements, shown in Fig. 3. The figure shows the total hydrogen depth profiles for samples (a) without and (b) with an Al_2O_3 capping layer.

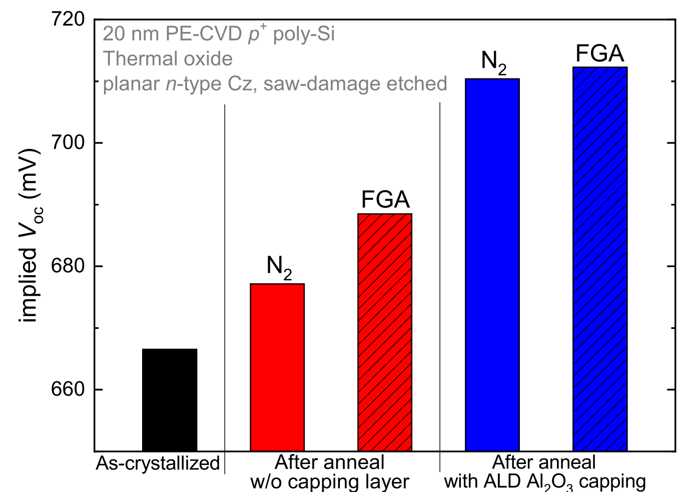

Fig. 2. The effect of the presence of an Al_2O_3 capping layer and annealing ambient on the implied open-circuit voltage for *n*-type Si passivated by p^+ poly-Si contact. Annealing was carried out for 1 h at 400 °C. Data are adapted from Schnabel et al. [30].

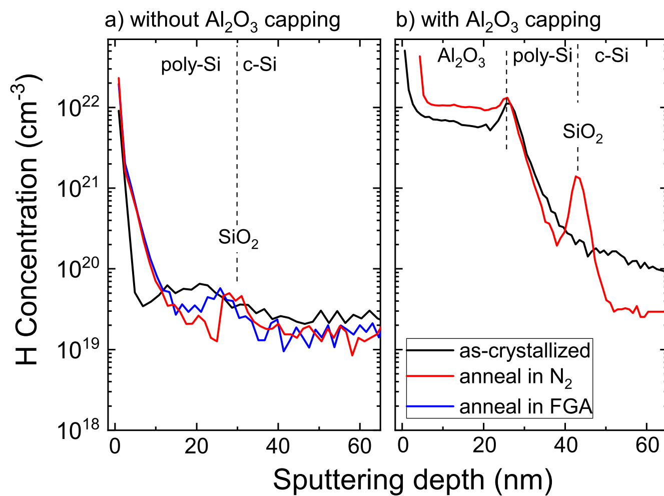

Fig. 3. Interface hydrogenation of poly-Si passivating contacts as studied by secondary ion-mass spectrometry. The poly-Si was prepared by PECVD, followed by SPC. Data are adapted from Schnabel et al. [30] For sake of clarity, the data from the original figure after forming gas annealing has been omitted from panel b).

Profiles are shown in the as-crystallized state and after annealing in either N_2 or a forming gas environment.

As can be seen (Fig. 3a), as-crystallized poly-Si features a low hydrogen concentration, and also at the *c*-Si/SiO_2 interface only low concentrations of hydrogen can be found. After annealing the poly-Si in N_2 or even forming gas, the hydrogen concentration near this interface remains similarly low. However, when the poly-Si is capped with Al_2O_3 – which typically contains 2–3 at. % of H [20] - a distinct peak in the hydrogen concentration appears near *c*-Si/SiO_2 surface after annealing in N_2 [20]. Our previous work with isotope labeling experiments has demonstrated that the hydrogen that is present near the c-Si/SiO_2 interface at least partially originates from the Al_2O_3 capping layer [30]. The presence of this hydrogen near this interface correlates with the increment in the surface passivation level of Fig. 2. This passivation level is enhanced because the H provides so-called chemical passivation, i.e., it reduces the interface defect density. It should be noted that the role of H in improving the *chemical* passivation of interfaces is not exclusive to SiO_2/poly-Si contacts, as similar observations have been made for example for the *c*-Si/SiO_2/Al_2O_3, *c*-Si/SiO_2/poly-SiC_x and *c*-Si/SiO_2/ZnO/Al_2O_3 systems [20,31,32].

4. Thermal stability and reversibility of poly-Si hydrogenation

In addition to providing hydrogenation of the poly-Si passivating contact, there are also a few other useful aspects to the use of dielectrics. Firstly, the presence of a dielectric capping layer can strongly enhance the thermal stability. Fig. 4 shows the iV_{oc} for symmetrical *n*-type lifetime samples that have been passivated by PE-CVD p^+ poly-Si. After crystallization, the poly-Si samples with and without a 30 nm ALD Al_2O_3 capping layer have been subjected to a forming gas anneal at 400 °C. For both sample types the passivation quality is observed to improve, with the strongest enhancement for the sample capped by ALD Al_2O_3. When exposing the same samples consecutively to higher annealing temperatures in N_2, the iV_{oc} immediately drops for the sample without an Al_2O_3 capping layer. However, in the presence of such a capping layer, the iV_{oc} remains stable and even increases slightly for annealing temperatures up

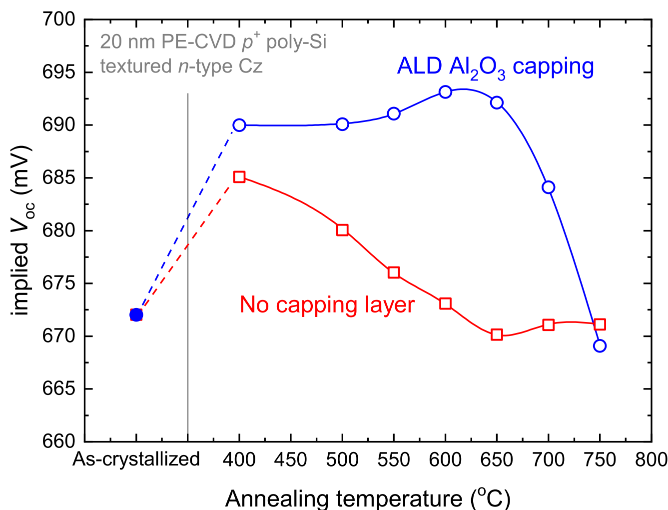

Fig. 4. Temperature stability of the passivation induced by p^+ poly-Si with and without a 30 nm ALD Al_2O_3 capping layer. The symmetrical lifetime samples have been subjected to consecutive anneals of 10 min.

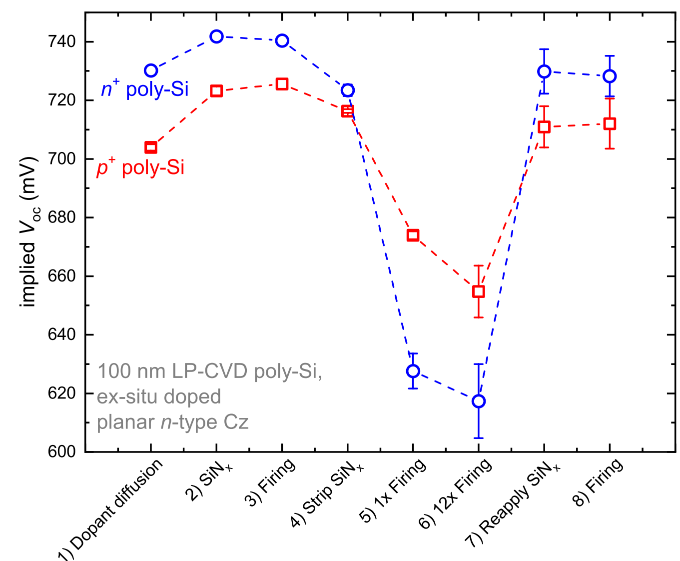

Fig. 5. Experiment showing the stability and reversibility of hydrogenation for symmetrical lifetime samples capped with *n*- or *p*-type poly-Si. Implied open-circuit voltage is measured at several instances, i.e., for as-prepared poly-Si (1), which subsequently has been capped by SiN_x (2), followed by a high-temperature firing step (3). Next, the SiN_x is stripped from the poly-Si by HF (4), and the sample is again fired for one (5) or multiple times (6). Next, a new SiN_x capping layer is deposited on the poly-Si sample (7), followed by a firing step (8). The error bars denote the standard deviation of five measurements on different parts of the wafer.

to 650 °C. Apparently, the Al_2O_3 can retain the hydrogen within the underlying SiO_2/poly-Si stack by supplying hydrogen and preventing the effusion of hydrogen. At annealing temperatures above 650 °C, the passivation for samples with an Al_2O_3 capping layer deteriorates. This can be explained by the fact that at this temperature, effusion of molecular hydrogen from the Al_2O_3 takes place [20], which most likely impairs its function as an effusion barrier. Naturally, it can be expected that the final passivation quality will not only depend on the anneal temperature, but also on the (total) anneal time, as is also the case with e.g., Al_2O_3 surface passivation layers [33]. The use of dielectrics for enhancing the thermal stability of passivation layers is also not unique for the SiO_2/poly-Si stack. For example, SiN_x has been shown to enhance the thermal stability of *a*-Si:H passivation layers significantly, up to 500 °C [34].

Secondly, the dielectric can be used as a *sacrificial* hydrogenation source and thirdly, the process of hydrogenation is *reversible* [35]. These two aspects are demonstrated in Fig. 5 for the case of a 75 nm PE-CVD SiN_x capping layer on both n^+ and p^+ poly-Si prepared by LP-CVD. As the figure shows, the application of the SiN_x dielectric enhances the passivation of the as-prepared poly-Si, reaching an outstanding iV_{oc} of 741 mV for n^+ poly-Si and 726 mV for p^+ poly-Si. Note that in this case the hydrogenation of the poly-Si takes place during the deposition of the SiN_x dielectric layer, most likely due to the higher deposition temperature of 375 °C as compared to the 200 °C for ALD Al_2O_3. Moreover, the passivation is quite resilient to the subsequent ~800 °C firing step. The fact that the SiN_x can be used as a *sacrificial* layer is evidenced by the only minor decrease in iV_{oc} after stripping the SiN_x from the poly-Si by prolonged soaking in hydrofluoric acid (HF). Note that this small decrease in iV_{oc} is not per se due to a reduction in passivation quality, but can (partially) stem from a reduction in light-coupling after removal of the SiN_x antireflection coating. Similarly, ALD Al_2O_3 has previously been shown to act as a suitable sacrificial hydrogenation layer on top of SiO_2/poly-Si and on thermally-grown SiO_2 [20,36].

After stripping the SiN_x, the passivation scheme is no longer stable under firing conditions, as evidenced by the steep decrease in iV_{oc} upon repeated firing. Interestingly, when redepositing a SiN_x on the poly-Si, the passivation is almost fully recovered and the stack is stable under firing conditions again. This notion of *reversibility* is particularly interesting from a processing point of view, as it means that even though the passivation through hydrogen might be lost during a certain high-temperature processing step (such as during dopant activation for in-situ doped poly-Si), it can in principle be reintroduced in a following processing step. For example, Naber *et al.* rely on this principle in a TOPCon solar cell process flow [14].

5. The effect of the doping level of the poly-Si

The extent of surface passivation in general relies on a combination of *chemical* passivation, i.e. the reduction of surface defect states, and *field-effect* passivation, which arises from induced band-bending at the *c*-Si interface [37]. In the case of poly-Si contacts, the high level of *chemical* passivation originates from the hydrogenated *c*-Si/SiO_x interface, as has been discussed in section 2, whereas the *field-effect* passivation originates from heavy doping of the poly-Si. This doping shifts the Fermi level in the poly-Si, leading to a work function difference between the *c*-Si wafer and the poly-Si. Heavy doping of the poly-Si is therefore generally beneficial for surface passivation, provided that excessive dopant in-diffusion through the SiO_2 into the wafer is avoided, which would otherwise lead to enhanced Auger recombination.

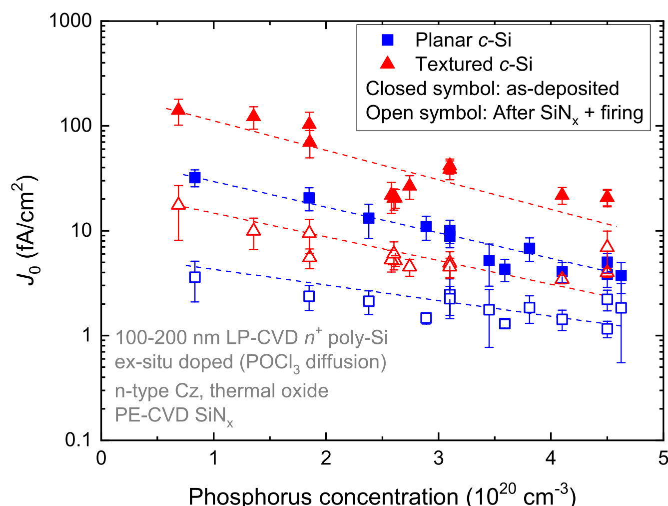

Fig. 6. Recombination parameter of n^+ poly-Si passivating contacts as a function of the phosphorus doping concentration in the poly-Si, before and after hydrogenation induced by the deposition of SiN_x and a subsequent high-temperature firing step. The lines are guides to the eye. Data are adapted from Stodolny *et al.* [10].

The beneficial effect of heavy (*n*-type) doping on the passivation quality is shown in Fig. 6. As can be seen, the recombination current density, J_0, decreases with increasing doping level of the poly-Si, both for planar and textured wafers. In all cases, hydrogenation by the deposition of a SiN_x dielectric layer and subsequent firing improves the surface passivation further. Although for very highly doped poly-Si contacts, i.e., with a strong *field-effect* passivation, hydrogenation is less crucial, yet it still helps in reducing the J_0 and to reach recombination current densities well below 10 fA/cm^2. For lowly-doped or intrinsic poly-Si, proper hydrogenation appears to be more critical due to the absence of significant field-effect passivation.

In the context of field-effect passivation, it is also instructive to consider the role of *field-effect* passivation provided by the fixed charge in the dielectrics used for hydrogenation. For instance, the SiN_x and Al_2O_3 dielectrics discussed so far are known to exhibit positive and negative fixed charge, respectively when deposited on silicon [38,39]. These fixed charge polarities should render Al_2O_3 suitable for enhancing the passivation of p^+ poly-Si contacts, whereas SiN_x should be more suited for n^+ poly-Si contacts. However, since the doped poly-Si layer is typically made thicker than the Debye length therein in order to make a selective contact, the effect of any fixed charge on the band bending at the *c*-Si interface will be screened. For example, for highly doped poly-Si with a doping density of $N_d = 10^{20}$ cm^{-3}, the screening length is only 0.4 nm. Therefore, the effect of fixed charge in the dielectric capping layer is expected not to play any role for carrier-selective, highly doped poly-Si contacts. However, for thin poly-Si passivation layers with a lower doping density, such as can be of interest on the front side of solar cells, the fixed charge in the dielectric capping layer could in principle play a role in the field-effect passivation.

6. Hydrogenation of poly-Si in solar cells

For wide-scale implementation of poly-Si passivating contacts in solar cell manufacturing it is desirable that the c-Si surface passivation provided by poly-Si is maintained after the high-temperature firing step, which is commonly used in solar cell production for metallization. To study the stability against the firing step in more detail, Fig. 7 compares the passivation level for 6 nm spatial ALD Al_2O_3 and 75 nm SiN_x single layers and stacks thereof on top of 200 nm LP-CVD p^+ poly-Si, for different firing temperatures. To prevent blistering, the Al_2O_3 thin films were annealed in nitrogen ambient at 425 °C for 20 min prior to subsequent SiN_X deposition or firing. As can be seen, the Al_2O_3 single layer yields high levels of passivation before firing, but exhibits relatively poor thermal stability after firing. The hydrogenation from the SiN_x single layer is, on the other hand, activated after firing and is more thermally stable. However, the use of an Al_2O_3/SiN_x layer stack provides the best passivation, in particular at higher firing temperatures. This is thought to originate from the combination of very effective hydrogenation from Al_2O_3 with the thick SiN_x layer acting as a dense capping layer that is stable under firing conditions. These results demonstrate that both the dielectric layer stack and the firing conditions matter when aiming to reach high levels of surface passivation.

It is emphasized that dielectrics used as capping layer for poly-Si can serve more purposes in solar cells than enabling hydrogenation of poly-Si contacts alone. For instance, when poly-Si is employed at the rear side of bifacial solar cells, a SiN_x capping layer can also serve as an anti-reflection coating to enhance the bifaciality. Naturally, another purpose of the dielectric capping layers can, in certain solar cell configurations, also be the direct surface passivation of the c-Si. The dielectric layers can thus be used for hydrogenation of the poly-Si contacts while also passivating parts of the c-Si which are not contacted with poly-Si. For example, this can be the case in poly-Si IBC solar cell configurations that feature gaps between the n^+ and p^+ poly-Si fingers, or when applying poly-Si contacts selectively below the metal fingers at the front side of PERC/nPERT solar cells.

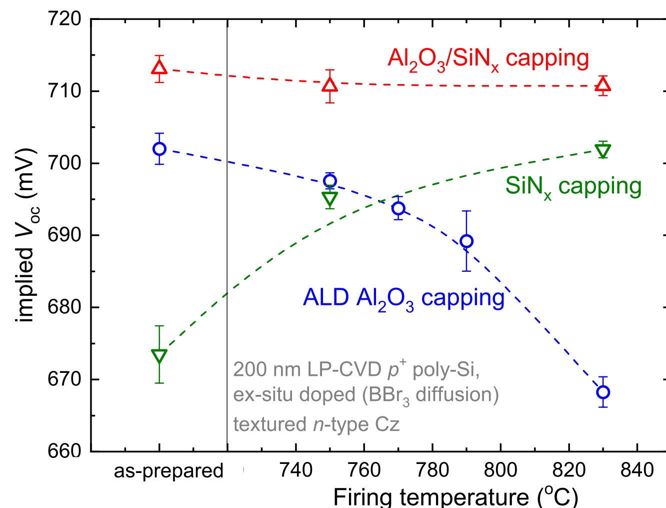

Fig. 7. Passivation levels obtained by p^+ poly-Si on textured *n*-type Cz by Al_2O_3, SiN_x, or Al_2O_3/SiN_x in combination with an industrially applied high-temperature anneal step ('firing'). Data are adapted from Mewe *et al.* [40] The error bars denote the standard deviation of five measurements on different parts of the wafer.

7. Conclusions

Several important aspects of the hydrogenation of poly-Si passivating contacts by dielectric layers have been addressed. It has been shown that dielectric capping layers, such as Al_2O_3, SiN_x or Al_2O_3/SiN_x stacks are very effective to further enhance the surface passivation offered by poly-Si, as they provide additional hydrogen to the *c*-Si/SiO_2 interface. After the hydrogenation step, the dielectric can be removed without impairing the improved passivation. Yet, it is advantageous to maintain the dielectric capping layer on the poly-Si as it enhances the thermal stability of the passivating stack. Moreover, it is shown that hydrogenation by dielectrics is beneficial for surface passivation regardless of the poly-Si doping level, albeit that its effect is more pronounced for more lowly-doped poly-Si samples as they exhibit lower levels of field-effect passivation. Depending on the specific solar cell architecture and process flow used, hydrogenation of poly-Si can be realized best by either Al_2O_3 or SiN_x layers, or by Al_2O_3 and SiN_x based stacks. In any case, optimization of the hydrogenation of poly-Si aids in achieving poly-Si contacts with excellent passivation quality.

Declaration of competing interest

The authors declare the following financial interests/personal relationships which may be considered as potential competing interests:

1. B.W.H. van de Loo is currently employed at SoLayTec, an ALD equipment supplier for photovoltaic industries.

CRediT authorship contribution statement

Bas W.H. van de Loo: Conceptualization, Writing - original draft, Visualization. **Bart Macco:** Conceptualization, Writing - original draft, Visualization. **Manuel Schnabel:** Investigation, Writing - review & editing, Investigation, Writing - review & editing. **Agnes A. Mewe:** Investigation, Writing - review & editing. **David L. Young:** Investigation, Writing - review & editing. **William Nemeth:** Investigation, Writing - review & editing. **Paul Stradins:** Investigation, Writing - review & editing. **Wilhelmus M.M. Kessels:** Conceptualization, Funding acquisition, Project administration, Writing - review & editing.

Acknowledgements

The authors acknowledge J. J. L. M. Meulendijks, C. O. van Bommel, C.A.A. van Helvoirt, J. van Gerwen and J. J. A. Zeebregts for their technical support. The authors gratefully acknowledge Solliance for funding the TEM facility. We acknowledge financial support for this research from the Top consortia for Knowledge and Innovation (TKI) Solar Energy programs RADAR (TEUE116905), AAA (1409104), IBC-sense (TEZ0214004), Miracle (TEUE116139), NexPas (TEZ0214002) and Antilope (TEID215011) of the Ministry of Economic Affairs of The Netherlands.

References

[1] A. Richter, J. Benick, F. Feldmann, A. Fell, M. Hermle, S.W. Glunz, n-Type Si solar cells with passivating electron contact: identifying sources for efficiency limitations by wafer thickness and resistivity variation, Sol. Energy Mater. Sol. Cells (2017) 1–10, https://doi.org/10.1016/j.solmat.2017.05.042.

[2] F. Haase, C. Hollemann, S. Schäfer, A. Merkle, M. Rienäcker, J. Krügener, R. Brendel, R. Peibst, Laser contact openings for local poly-Si-metal contacts enabling 26.1%-efficient POLO-IBC solar cells, Sol. Energy Mater. Sol. Cells 186 (2018) 184–193, https://doi.org/10.1016/j.solmat.2018.06.020.

[3] Y. Chen, D. Chen, C. Liu, Z. Wang, Y. Zou, Y. He, Y. Wang, L. Yuan, J. Gong, W. Lin, X. Zhang, Y. Yang, H. Shen, Z. Feng, P.P. Altermatt, P.J. Verlinden, Mass production of industrial tunnel oxide passivated contacts (i-TOPCon) silicon solar

cells with average efficiency over 23% and modules over 345 W, Prog. Photovoltaics Res. Appl. (2019) 3180, https://doi.org/10.1002/pip.3180, pip.
[4] J. Melskens, B.W.H. van de Loo, B. Macco, L.E. Black, S. Smit, W.M.M. Kessels, Passivating contacts for crystalline silicon solar cells: from concepts and materials to prospects, IEEE J. Photovoltaics. 8 (2018) 373–388, https://doi.org/10.1109/JPHOTOV.2018.2797106.
[5] R. Brendel, R. Peibst, Contact selectivity and efficiency in crystalline silicon photovoltaics, IEEE J. Photovoltaics. 6 (2016) 1413–1420, https://doi.org/10.1109/JPHOTOV.2016.2598267.
[6] C. Hollemann, F. Haase, S. Schäfer, J. Krügener, R. Brendel, R. Peibst, 26.1%-efficient POLO-IBC cells: quantification of electrical and optical loss mechanisms, Prog. Photovoltaics Res. Appl. (2019) 1–9, https://doi.org/10.1002/pip.3098.
[7] A. Moldovan, F. Feldmann, M. Zimmer, J. Rentsch, J. Benick, M. Hermle, Tunnel oxide passivated carrier-selective contacts based on ultra-thin SiO2 layers, Sol. Energy Mater. Sol. Cells 142 (2015) 123–127, https://doi.org/10.1016/j.solmat.2015.06.048.
[8] R. van der Vossen, F. Feldmann, A. Moldovan, M. Hermle, Comparative study of differently grown tunnel oxides for p-type passivating contacts, Energy Procedia 124 (2017) 448–454, https://doi.org/10.1016/j.egypro.2017.09.273.
[9] B. Nemeth, D.L. Young, M.R. Page, V. LaSalvia, S. Johnston, R. Reedy, P. Stradins, Polycrystalline silicon passivated tunneling contacts for high efficiency silicon solar cells, J. Mater. Res. 31 (2016) 671–681, https://doi.org/10.1557/jmr.2016.77.
[10] M.K. Stodolny, J. Anker, B.L.J. Geerligs, G.J.M. Janssen, B.W.H. Van De Loo, J. Melskens, R. Santbergen, O. Isabella, J. Schmitz, M. Lenes, J.M. Luchies, W.M. M. Kessels, I. Romijn, Material properties of LPCVD processed n-type polysilicon passivating contacts and its application in PERPoly industrial bifacial solar cells, Energy Procedia 124 (2017) 635–642, https://doi.org/10.1016/j.egypro.2017.09.250.
[11] D.L. Young, W. Nemeth, V. Lasalvia, M.R. Page, S. Theingi, M. Young, J. Aguiar, B. G. Lee, P. Stradins, Plasma immersion ion implantation for interdigitated back passivated contact (IBPC) solar cells, 2017, IEEE 44th Photovolt. Spec. Conf. PVSC 158 (2017) 1–5, https://doi.org/10.1109/PVSC.2017.8366532, 2017.
[12] C. Reichel, F. Feldmann, R. Müller, R.C. Reedy, B.G. Lee, D.L. Young, P. Stradins, M. Hermle, S.W. Glunz, Tunnel oxide passivated contacts formed by ion implantation for applications in silicon solar cells, J. Appl. Phys. 118 (2015), https://doi.org/10.1063/1.4936223.
[13] U. Römer, R. Peibst, T. Ohrdes, B. Lim, J. Krügener, T. Wietler, R. Brendel, Ion implantation for poly-Si passivated back-junction back-contacted solar cells, IEEE J. Photovolt. 5 (2015) 507–514, https://doi.org/10.1109/JPHOTOV.2014.2382975.
[14] R.C. Naber, B.W.H. van de Loo, J.M. Luchies, LPCVD in-situ n-type doped poly-silicon process throughput optimization and implementation into an industrial solar cell process flow, Proc. 34th Eur. Photovolt. Sol. Energy Conf. 53 (2019).
[15] A. Aberle, S. Glunz, W. Warta, J. Kopp, J. Knobloch, SiO_2-passivated high efficiency silicon solar cells: process dependence of Si-SiO_2 interface recombination, in: Tenth E.C. Photovolt. Sol. Energy Conf., Springer Netherlands, Dordrecht, 1991, pp. 631–635, https://doi.org/10.1007/978-94-011-3622-8_161.
[16] F. Feldmann, M. Bivour, C. Reichel, H. Steinkemper, M. Hermle, S.W. Glunz, Tunnel oxide passivated contacts as an alternative to partial rear contacts, Sol. Energy Mater. Sol. Cells 131 (2014) 46–50, https://doi.org/10.1016/j.solmat.2014.06.015.
[17] F. Feldmann, C. Reichel, R. Müller, M. Hermle, The application of poly-Si/SiO_x contacts as passivated top/rear contacts in Si solar cells, Sol. Energy Mater. Sol. Cells 159 (2017) 265–271, https://doi.org/10.1016/j.solmat.2016.09.015.
[18] M.K. Stodolny, M. Lenes, Y. Wu, G.J.M. Janssen, I.G. Romijn, J.R.M. Luchies, L. J. Geerligs, n-Type polysilicon passivating contact for industrial bifacial n-type solar cells, Sol. Energy Mater. Sol. Cells 158 (2016) 24–28, https://doi.org/10.1016/j.solmat.2016.06.034.
[19] L. Tutsch, F. Feldmann, B. Macco, M. Bivour, E. Kessels, M. Hermle, Improved passivation of n-type poly-Si based passivating contacts by the application of hydrogen-rich transparent conductive oxides, IEEE J. Photovolt. (2020) 1–6, https://doi.org/10.1109/JPHOTOV.2020.2992348.
[20] G. Dingemans, W. Beyer, M.C.M. van de Sanden, W.M.M. Kessels, Hydrogen induced passivation of Si interfaces by Al_2O_3 films and SiO_2/Al_2O_3 stacks, Appl. Phys. Lett. 97 (2010), https://doi.org/10.1063/1.3497014, 152106.
[21] T.N. Truong, D. Yan, W. Chen, M. Tebyetekerwa, M. Young, M. Al-Jassim, A. Cuevas, D. Macdonald, H.T. Nguyen, Hydrogenation mechanisms of poly-Si/SiO_x passivating contacts by different capping layers, Sol. RRL. 4 (2020), https://doi.org/10.1002/solr.201900476, 1900476.
[22] Y. Yang, P.P. Altermatt, Y. Cui, Y. Hu, D. Chen, L. Chen, G. Xu, X. Zhang, Y. Chen, P. Hamer, R.S. Bonilla, Z. Feng, P.J. Verlinden, Effect of carrier-induced hydrogenation on the passivation of the poly-Si/SiO_x/c-Si interface, AIP Conf. Proc. 1999 (2018), https://doi.org/10.1063/1.5049289.
[23] T. Truong, D. Yan, A. Cuevas, D. MacDonald, H.T. Nguyen, Hydrogenation of polycrystalline silicon films for passivating contacts solar cells, Conf. Rec. IEEE Photovolt. Spec. Conf. (2019) 2705–2708, https://doi.org/10.1109/PVSC40753.2019.8980647.
[24] T.N. Truong, D. Yan, C. Samundsett, A. Liu, S.P. Harvey, M. Young, Z. Ding, M. Tebyetekerwa, F. Kremer, M. Al-Jassim, A. Cuevas, D. MacDonald, H.T. Nguyen, Hydrogen-assisted defect engineering of doped poly-Si films for passivating contact solar cells, ACS Appl. Energy Mater. 2 (2019) 8783–8791, https://doi.org/10.1021/acsaem.9b01771.
[25] J. Temmler, J.I. Polzin, F. Feldmann, L. Kraus, B. Kafle, S. Mack, A. Moldovan, M. Hermle, J. Rentsch, Inline PECVD deposition of poly-Si-based tunnel oxide passivating contacts, Phys. Status Solidi Appl. Mater. Sci. 215 (2018) 1–4, https://doi.org/10.1002/pssa.201800449.
[26] S. Duttagupta, N. Nandakumar, P. Padhamnath, J.K. Buatis, R. Stangl, A.G. Aberle, monoPoly™ cells: large-area crystalline silicon solar cells with fire-through screen printed contact to doped polysilicon surfaces, Sol. Energy Mater. Sol. Cells 187 (2018) 76–81, https://doi.org/10.1016/j.solmat.2018.05.059.
[27] Z. Rui, Y. Zeng, X. Guo, Q. Yang, Z. Wang, C. Shou, W. Ding, J. Yang, X. Zhang, Q. Wang, H. Jin, M. Liao, S. Huang, B. Yan, J. Ye, On the passivation mechanism of poly-silicon and thin silicon oxide on crystal silicon wafers, Sol. Energy 194 (2019) 18–26, https://doi.org/10.1016/j.solener.2019.10.064.
[28] G. Yang, A. Ingenito, O. Isabella, M. Zeman, IBC c-Si solar cells based on ion-implanted poly-silicon passivating contacts, Sol. Energy Mater. Sol. Cells 158 (2016) 84–90, https://doi.org/10.1016/j.solmat.2016.05.041.
[29] D.E. Kane, R.M. Swanson, Measurement of the emitter saturation current by a contactless photoconductivity decay method, in: 18th IEEE Photovolt. Spec. Conf., Las Vegas, 1985, p. 578.
[30] M. Schnabel, B.W.H. van de Loo, W. Nemeth, B. Macco, P. Stradins, W.M. M. Kessels, D.L. Young, Hydrogen passivation of poly-Si/SiO_x contacts for Si solar cells using Al_2O_3 studied with deuterium, Appl. Phys. Lett. 112 (2018), https://doi.org/10.1063/1.5031118, 203901.
[31] B.W.H. van de Loo, B. Macco, J. Melskens, W. Beyer, W.M.M. Kessels, Silicon surface passivation by transparent conductive zinc oxide, J. Appl. Phys. 125 (2019), https://doi.org/10.1063/1.5054166, 105305.
[32] M. Lehmann, N. Valle, J. Horzel, A. Pshenova, P. Wyss, M. Döbeli, M. Despeisse, S. Eswara, T. Wirtz, Q. Jeangros, A. Hessler-Wyser, F.-J. Haug, A. Ingenito, C. Ballif, Analysis of hydrogen distribution and migration in fired passivating contacts (FPC), Sol. Energy Mater. Sol. Cells 200 (2019), https://doi.org/10.1016/j.solmat.2019.110018, 110018.
[33] A. Richter, J. Benick, M. Hermle, S.W. Glunz, Reaction kinetics during the thermal activation of the silicon surface passivation with atomic layer deposited Al_2O_3, Appl. Phys. Lett. 104 (2014), 061606, https://doi.org/10.1063/1.4865901.
[34] S. Gatz, H. Plagwitz, P.P. Altermatt, B. Terheiden, R. Brendel, Thermal stability of amorphous silicon/silicon nitride stacks for passivating crystalline silicon solar cells, Appl. Phys. Lett. 93 (2008), https://doi.org/10.1063/1.3009571, 173502.
[35] M. Lozac'h, S. Nunomura, H. Umishio, T. Matsui, K. Matsubara, Roles of hydrogen atoms in p-type Poly-Si/SiO_x passivation layer for crystalline silicon solar cell applications, Jpn. J. Appl. Phys. 58 (2019), 050915, https://doi.org/10.7567/1347-4065/ab14fe.
[36] M. Schnabel, B.W.H. Van De Loo, W. Nemeth, B. Macco, P. Stradins, W.M. M. Kessels, D.L. Young, Hydrogen passivation of poly-Si/SiO_x contacts for Si solar cells using Al_2O_3studied with deuterium, Appl. Phys. Lett. 112 (2018), https://doi.org/10.1063/1.5031118.
[37] A. Cuevas, Y. Wan, D. Yan, C. Samundsett, T. Allen, X. Zhang, J. Cui, J. Bullock, Carrier population control and surface passivation in solar cells, Sol. Energy Mater. Sol. Cells 184 (2018) 38–47, https://doi.org/10.1016/j.solmat.2018.04.026.
[38] G. Dingemans, W.M.M. Kessels, Status and prospects of Al_2O_3-based surface passivation schemes for silicon solar cells, J. Vac. Sci. Technol. Vac. Surf. Film. 30 (2012), 040802, https://doi.org/10.1116/1.4728205.
[39] A. Cuevas, T. Allen, J. Bullock, Yimao Wan, Xinyu Zhang, Skin care for healthy silicon solar cells, Di, in: 2015 IEEE 42nd Photovolt. Spec. Conf., IEEE, 2015, pp. 1–6, https://doi.org/10.1109/PVSC.2015.7356379.
[40] A. Mewe, M. Stodolny, J. Anker, M. Lenes, X. Pagès, Y. Wu, K. Tool, B. Geerligs, I. Romijn, Full wafer size IBC cell with polysilicon passivating contacts, AIP Conf. Proc. 1999 (2018), https://doi.org/10.1063/1.5049277.